

Mechanistic Insights into Structural Stability of the Selectivity Filters in Typical Cation Channels

Zhoubin Tang, Hu Qiu, Wanlin Guo*

Key Laboratory for Intelligent Nano Materials and Devices of the Ministry of Education, State Key Laboratory of Mechanics and Control of Mechanical Structure, College of Aerospace Engineering, Nanjing University of Aeronautics and Astronautics, Nanjing, China

Email: *wlguo@nuaa.edu.cn

How to cite this paper: Tang, Z.B., Qiu, H. and Guo, W.L. (2022) Mechanistic Insights into Structural Stability of the Selectivity Filters in Typical Cation Channels. *Journal of Materials Science and Chemical Engineering*, 10, 17-32.

<https://doi.org/10.4236/msce.2022.107002>

Received: May 30, 2022

Accepted: July 26, 2022

Published: July 29, 2022

Abstract

The reliable functioning of ion channels should be closely related to their structural stability. The selectivity filter in the KcsA potassium channel possesses four stable ion binding sites that can coordinate nearly fully dehydrated ions, whereas only two of such binding sites exist in the non-selective NaK channel, and none of them is found in the NavAb sodium channel. Here we show that the stability of the selectivity filters in these tetrameric cation channels is inversely correlated with the number of stable binding sites by extensive molecular dynamics simulations. While the presence of coordinated ions is crucial for the selectivity filters of the KcsA and NaK channels to stabilize the conformations in their crystal structures, the selectivity filter of the NavAb channel shows higher stability, independent of the presence of ions. We further show that the distinct repulsive electrostatic interactions between negatively charged oxygen atoms in the selectivity filter which form the stable binding sites are responsible for the different stability of these cation channels. The hydrogen bonding networks between residues in the selectivity filter and its adjacent pore helix also play an important role in maintaining stability. Together, these results provide important mechanistic insights into the structural stability of the selectivity filters in typical cation channels.

Keywords

Ion Channel, Structural Stability, Molecular Dynamics, Electrostatic Potential, Hydrogen Bonds

1. Introduction

The study of the structure-function relationship of proteins is essential for un-

derstanding living systems. Voltage-gated cation channels, especially the potassium and sodium ion channels, play an important role in numerous physiological processes such as the propagation of action potentials [1]. Although more and more structures of ion channels have been experimentally resolved, it remains challenging to understand the structure-function relationship from an evolutionary point of view. It is especially attractive to find that the structural evolution from potassium channels to sodium channels is huge, especially in the selectivity filter regimes. The filter of the tetrameric KcsA channel and most other K⁺ channels contain a narrow pore constituted by the highly conserved amino acid sequence motif TVGYG in a four-fold symmetric arrangement [2] [3]. The backbone carbonyl oxygen atoms and the threonine hydroxyl group lining the narrow pore of the selectivity filter form altogether four stable K⁺ binding sites that can coordinate nearly fully dehydrated ions, called S1 to S4 from the extracellular side (**Figure 1(A)**) [4] [5]. Different from KcsA, the selectivity filter of the non-selective NaK channel, with a characteristic sequence of TVGDG, has only two of such binding sites (S3 and S4), along with a vestibule in the region corresponding to the first two binding sites (S1 and S2) in KcsA (**Figure 1(B)**) [6]. In sharp contrast to K⁺ and NaK channels, the selectivity filter in sodium channels such as the NavAb bacterial sodium channel displays a totally different structure, without any such stable binding sites that can coordinate nearly fully dehydrated ions (**Figure 1(C)**) [7].

It was proposed that the presence of coordinated K⁺ ions in the selectivity filter of a potassium channel is essential to maintaining its conductive conformation and therefore its function [8]. For instance, C-type inactivation of the KcsA channel is thought to involve a constriction of the selectivity filter [9], and the constricted conformation of the filter was first observed in a KcsA structure determined at low K⁺ concentration (PDB ID 1K4D) [5]. Compared with the structure at high K⁺ concentration, the carbonyl oxygen of Val76 at low K⁺ concentration is significantly tilted, and meanwhile, the filter narrows as a result of the inward movement of Gly77. Indeed, previous molecular dynamics (MD) simulations have found that the absence of K⁺ ions in the selectivity filter will distort the KcsA filter, leading to a conformation similar to the nonconductive conformation at low K⁺ concentration [10] [11] [12] [13] [14].

Likewise, the selectivity filter of the NaK channel also requires the presence of cations to maintain its structural stability, and the absence of cations will lead to structural changes in the selectivity filter [15] [16]. In sharp contrast, the selectivity filter of sodium channels such as NavAb is stable, and seemingly independent of the presence of Na⁺ ions, as noted in our previous MD simulations [17]. Among these three channels, the underlying mechanism for the structural stability of the KcsA channel has been widely studied [18]-[22]. However, there are few studies involving the stability mechanism of NaK and NavAb channels. For this reason, it remains difficult to provide a unified understanding of the structural stability of different ion channels from a mechanistic point of view.

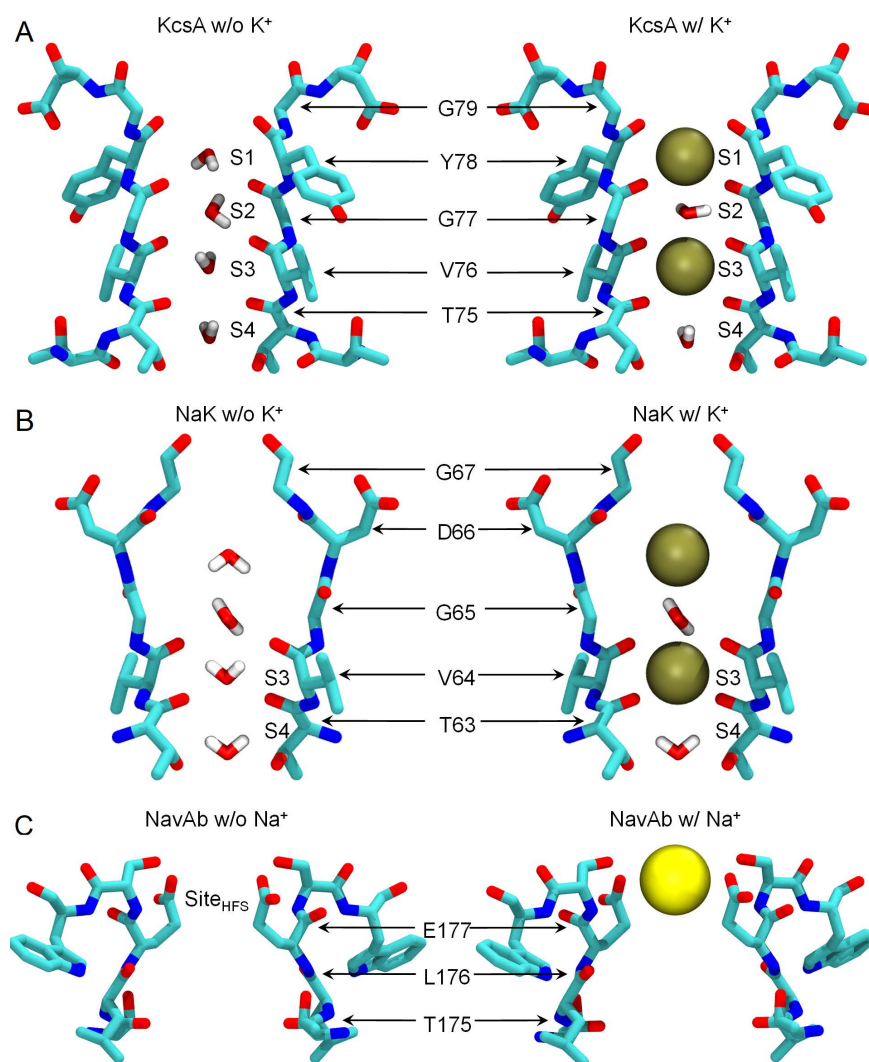


Figure 1. Overview of the simulation systems. (A) Structures of the KcsA selectivity filter occupied by solely water molecules (denoted as “KcsA w/o K⁺”) and by water in S2 and S4 plus K⁺ ions in S1 and S3 (denoted as “KcsA w/K⁺”). (B) Structures of the NaK selectivity filter occupied by solely water molecules (denoted as “NaK w/o K⁺”) and by water plus K⁺ ions (denoted as “NaK w/ K⁺”). (C) Structures of the NavAb channel with its selectivity filter occupied by solely water molecules (denoted as “NavAb w/o Na⁺”) and by water plus a Na⁺ ion (denoted as “NavAb w/Na⁺”). K⁺ and Na⁺ ions are represented as brown and yellow spheres, respectively. For visual clarity, only two subunits are shown in each case.

In this work, we compared the structural stability of the selectivity filters of KcsA, NaK and NavAb channels in the absence of ions by comprehensive MD simulations (**Figure 1**, left panels). The simulations yielded a detailed conformational change process occurring in the selectivity filters of KcsA and NaK, but revealed the high stability for the selectivity filter of NavAb. As a control, we also performed simulations on these channels in the presence of coordinated ions (**Figure 1**, right panels) and found no significant conformational changes for all three channels. Subsequent analyses on repulsive electrostatic forces and hydro-

gen bond networks in the selectivity filter region revealed the mechanism for the different stability of these cation channels.

2. Methods

2.1. Model Construction

MD simulations for the KcsA channel were conducted based on the crystal structure determined in a conductive conformation (PDB ID: 1K4C) [5]. Most residues were assigned to their standard protonation state at pH 7. The residue Glu71 was modelled in a protonated state to enable the formation of a key hydrogen bond with Asp80 [23] [24] [25]. The ion channel, with its symmetry axis aligned along the *z*-axis, was embedded in a POPC lipid bilayer. Water molecules were added to solvate the systems. K⁺ and Cl⁻ ions were added to the bulk solvent to reproduce experimental ionic concentrations (150 mM KCl) and to obtain the electric neutrality of the system. Then two simulation models shown in **Figure 1(A)** (denoted as “KcsA w/o K⁺” and “KcsA w/K⁺”) were constructed. The final systems contain roughly 86,200 atoms. Moreover, we also constructed molecular models based on the NaK channel (PDB ID: 2AHZ) [6] and NavAb sodium channel (PDB ID: 3RVY) [7], with a similar procedure as described above. For improving the computational efficiency, the voltage-sensing domain of the NavAb channel was removed.

2.2. MD Simulations

All MD simulations were carried out using NAMD2 [26], and visualized and analyzed with VMD [27]. The CHARMM36 force field was employed for protein [28] [29] [30], lipids [31] and ions [32]. The TIP3P model was used for describing water [33]. The long-range electrostatic interactions were computed using the particle mesh Ewald method [34]. A time step of 2 fs was used. All the simulations were performed in the NPT ensemble, whereby the temperature was maintained at 300 K by the Langevin thermostat, and the pressure was maintained at 1 atm by the Langevin piston pressure control [35].

After a 5000-step energy minimization, each system was simulated for 0.5 ns whereby all components except the lipid tails were fixed to remove the gap between the protein and lipid tails. Subsequently, a 1.6 ns pre-equilibration was carried out where a gradually decreasing harmonic constraint was applied to each protein atom. Finally, the production run was performed for 100 ns without any restraints. To avoid the influence of newly inserted ions into the selectivity filter, a fictive wall was applied to repel ions that approach the average *z* position of P atoms in lipids from the extracellular side of the membrane. The electrostatic potentials were computed with the PMEpot plugin of VMD [36]. In our simulations, a hydrogen bond is considered as being formed between an atom with a hydrogen bonded to it (donor, D) and another atom (acceptor, A), provided that the distance D-A is less than 3.5 Å and the angle D-H-A is less than 30°.

3. Results and Discussion

3.1. Stability of the Selectivity Filter

Figure 2 shows the root-mean-square deviation (RMSD) for the backbone atoms of the selectivity filters of the KcsA, NaK and NavAb channels as a function of simulation time with respect to the crystal structures. In the presence of coordinated ions, the RMSD values of all the three channels are always lower than 1.0 Å in the whole 100 ns MD simulation (**Figure 2(A)**), confirming the strong stability of the selectivity filters in these channels. In stark contrast, when ions are absent, the RMSD for the KcsA filter quickly exceeds 1.0 Å within 1 ns even when the whole protein is still constrained (black line in **Figure 2(B)**), and eventually fluctuates around ~1.8 Å. This result is consistent with previous works [10] [11] [12] [13] [14] and shows the worst stability of the KcsA filter among the three studied channels. The RMSD of the NaK filter quickly reaches and fluctuates around ~1.5 Å (red line in **Figure 2(B)**). However, the RMSD for the NavAb filter stays at ~0.5 Å (blue line in **Figure 2(B)**) during the 100 ns simulation even in the absence of Na⁺ ions, indicating its higher intrinsic stability as compared to KcsA and NaK. Considering the fact that there are four, two and zero stable ion bindings sites that can coordinate fully dehydrated ions in KcsA, NaK and NavAb filters [4] [5] [6] [7], respectively, it is interesting to note that the filter stability is inversely correlated with the number of stable binding sites in these three cation channels.

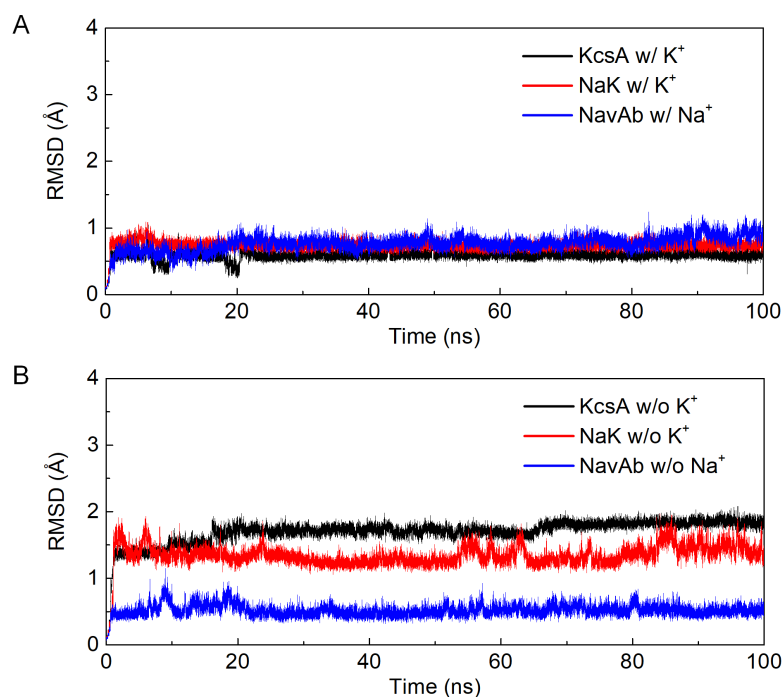


Figure 2. RMSD for all backbone atoms of the selectivity filter relative to the crystal structure in three cation channels during simulations with (A) and without (B) ions residing in the selectivity filter. Note that the protein underwent a gradually weakened constrain in the first 1.6 ns of each simulation (see Methods for details).

3.2. Conformational Change Process of KcsA and NaK Selectivity Filters

By inspecting the MD trajectory, we found that the conformational change (*i.e.*, the origin of the RMSD increase) of the KcsA channel in the absence of K^+ ions is mainly embodied in the flipping of the carbonyl oxygen of Val76, and the narrowing of the selectivity filter pore around Gly77 (**Figure 3**). The Val76 carbonyl oxygen, originally pointing toward the lumen to coordinate K^+ ion, undergoes a $\sim 180^\circ$ reorientation, namely, flipping away from the conduction pathway (marked with blue curved arrows). The narrowing of conduction pathway of the selectivity filter is caused by the inward movement of the α -carbon atom (C_α) of Gly77, which occludes the pore and makes it become a distinct “hourglass” shape (red arrows). In addition, we note that the flipping of Val76 occurs for all four subunits even in the initial pre-equilibration period (see the $t = 1.6$ ns snapshots) and lasts for the rest of time (**Figure 5(B)**). On the contrary, the narrowing of the filter around Gly77 occurs for only some of the four subunits (**Figure 5(E)**). For instance, at $t = 1.6$ ns, such narrowing only occurs in chain A and C, but not in chain B and D; it occurs in chain B at $t = 20$ ns, but does not appear in chain D during the whole 100 ns simulation. It is also striking that the narrowing in chain C disappears at $t = 94$ ns.

Similar to KcsA, the selectivity filter of the NaK channel also shows significant conformational change, as shown in **Figure 4**. The residue Val64 in the NaK channel, equivalent to Val76 in the KcsA channel, also undergoes flipping during

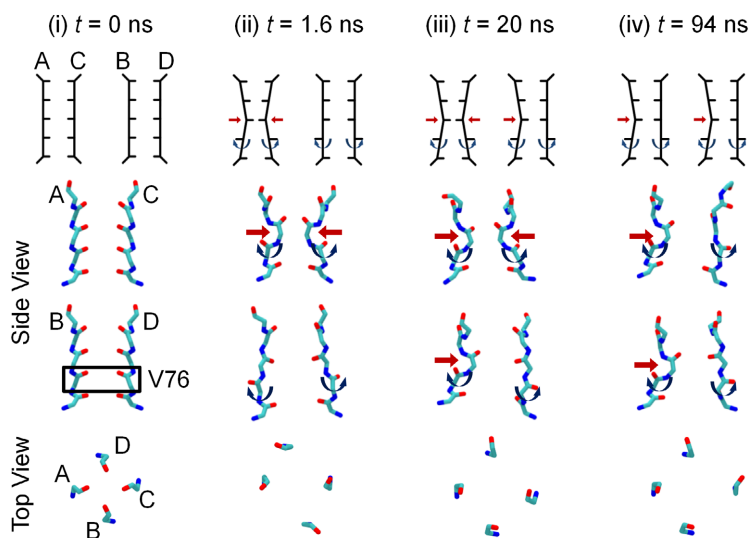


Figure 3. Conformational change process of the KcsA selectivity filter in the absence of K^+ ions (*i.e.*, based on the “KcsA w/o K^+ ” model). The top panel shows a schematic of the conformational change. The lower three panels show the snapshots of the selectivity filter backbone structures, from left to right, in the crystal structure ($t = 0$ ns), and in the simulation trajectory at $t = 1.6$ ns, 20 ns and 94 ns. The bottom panels show the top view of the backbone of Val76 from the extracellular side. The conformational change includes the flipping of the carbonyl oxygen of Val76 (blue arrows) and the narrowing of selectivity filter pore around Gly77 (red arrows).

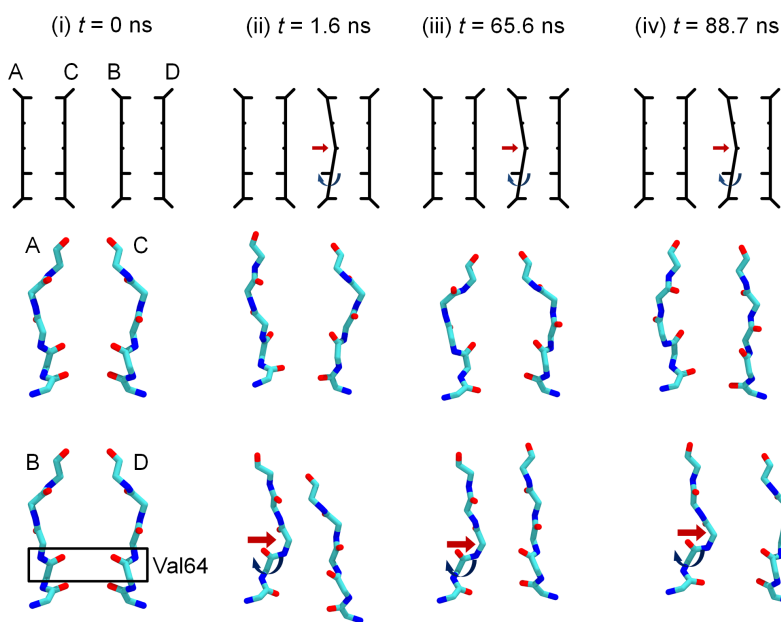


Figure 4. Conformational change process of the NaK selectivity filter in the absence of K^+ ions. The top panel shows a schematic of the conformational change. The lower two panels show the snapshots of the selectivity filter backbone structures, from left to right, in the crystal structure ($t = 0$ ns), and in the simulation trajectory at $t = 1.6$ ns, 65.6 ns and 88.7 ns. The conformational change process includes the flipping of the carbonyl oxygen of Val64 (blue arrows) and the narrowing of selectivity filter pore around Gly65 (red arrows).

the MD simulation (blue curved arrows). However, different from KcsA, such flipping does not occur in all four subunits, but instead, only in chain B. In addition, chain B also undergoes narrowing around Gly65, a residue equivalent to Gly77 in KcsA (red arrows). Such flipping and narrowing both occur within the initial pre-equilibration period and lasts for the rest of time (**Figure 5(C)** and **Figure 5(F)**). These results suggest that the NaK channel shares a similar conformational change process with that of the KcsA channel, but at a lower degree.

3.3. Repulsive Electrostatic Interactions in the Selectivity Filter Control the Stability

About four decades ago, Almers and Armstrong suggested that the repulsive electrostatic forces between negative charges or dipoles lining in the pore will destroy the pore structure of potassium channels [37]. Based on the available crystal structure, we now know that there exists four backbone carbonyl oxygen atoms and threonine side chain oxygen with electro-negativity in each subunit exposing toward the pore lumen in KcsA. It is natural to speculate that the presence of K^+ ions contributes to the overall stability of the selectivity filter by counterbalancing the repulsive electrostatic forces between the negatively charged oxygen atoms. Below we validate this hypothesis by measuring the electrostatic potential distribution in the KcsA channel and show that this mechanism is extendable to the NaK and NavAb channels (**Figure 6**).

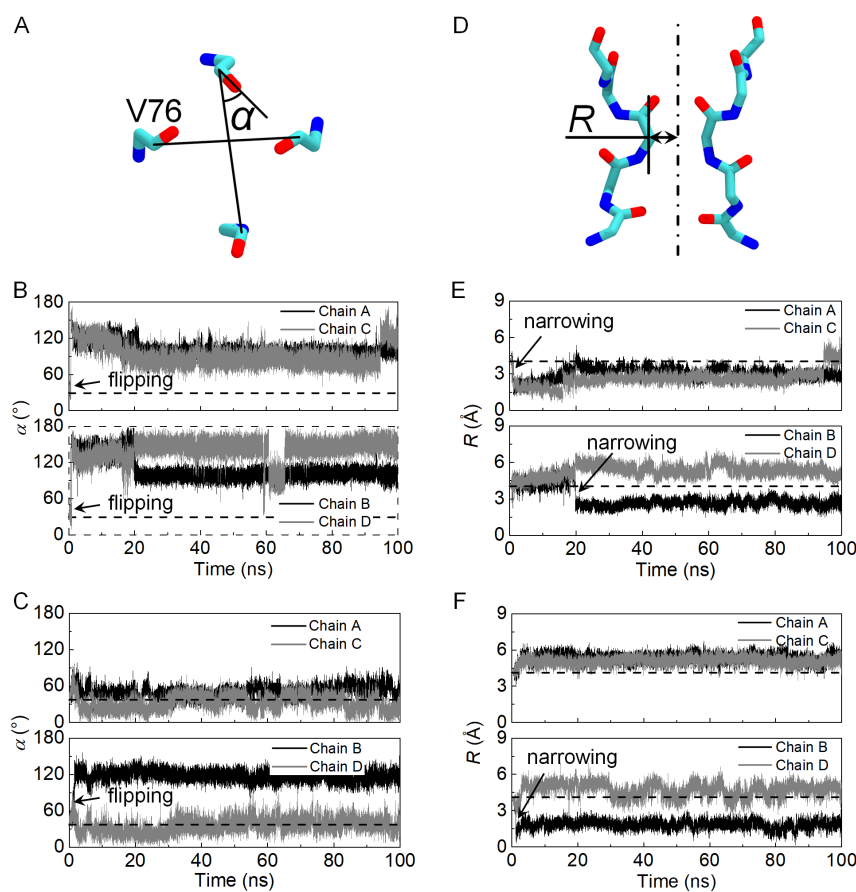


Figure 5. Flipping and narrowing of KcsA and NaK selectivity filters in the absence of K^+ ions. (A) Definition of α : take KcsA for example, α is defined as the acute angle between the axis of a carbonyl group and the line connecting the carbonyl carbon atoms in two diagonally opposed subunits. (B) Variation of the orientation angle α of the Val76 carbonyl oxygen in KcsA as a function of simulation time. (C) Variation of the orientation angle α of the Val64 carbonyl oxygen in NaK as a function of simulation time. (D) Definition of R : take KcsA for example, R is defined as the distance between the C α atom of Gly77 and the central axis of selectivity filter. (E) Local radius R around Gly77 in KcsA as a function of simulation time. (F) Local radius R around Gly65 in NaK as a function of simulation time. In panels (B), (C), (E) and (F), the value of α and R in crystal structure are indicated by dashed lines.

The average electrostatic potential maps along the x - z plane ($y = 0 \text{ \AA}$) inside the channel pores for KcsA in different three states are shown in **Figure 6(A)** to **Figure 6(C)**: in the absence of K^+ before flipping (“w/o K^+ , before flipping”), in the absence of K^+ after flipping (“w/o K^+ , after flipping”), and in the presence of K^+ (“w/ K^+ ”). The electrostatic potential changes along the channel axis in these systems are shown in **Figure 6(D)**. The electrostatic potentials in all three maps are uniform in bulk water regions away from the lipid membrane and the protein. However, difference arises between these maps particularly in the selectivity filter region. For instance, prior to the flipping of the Val76 carbonyl oxygen, there is a large and deep electrostatic potential valley in selectivity filter region (**Figure 6(A)** and **Figure 6(D)**). This electrostatic potential valley is caused by

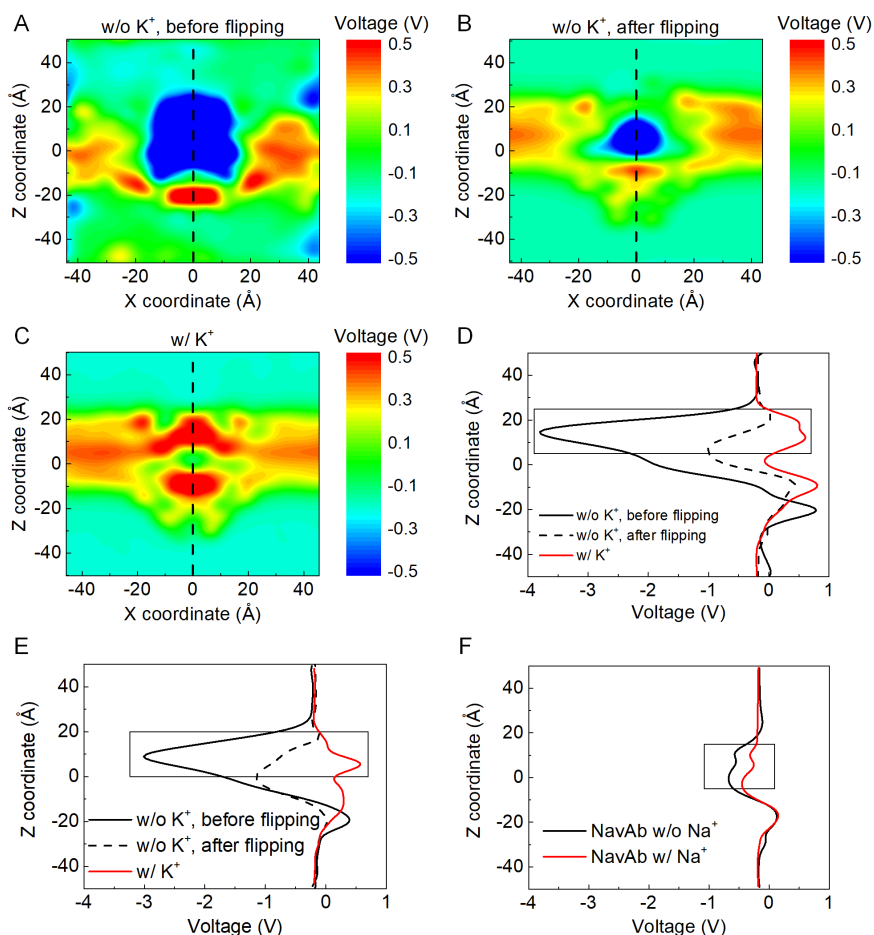


Figure 6. Electrostatic potential distributions. ((A)-(C)) Average electrostatic potential maps along the x - z plane ($y = 0$ Å) for KcsA in different states: in the absence of K^+ before flipping (“w/o K^+ , before flipping”), in the absence of K^+ after flipping (“w/o K^+ , after flipping”), and in the presence of K^+ (“w/ K^+ ”). (D) Electrostatic potential change along the channel axis of KcsA in each state (depicted as dash lines in panel (A)-(C)). (E) Electrostatic potential change along the channel axis of NavAb in three different states. (F) Electrostatic potential change along the channel axis of NavAb in two different states. The selectivity filter region is marked with rectangles.

the dense, negatively charged oxygen atoms of the backbone carbonyls. As a consequence, these negatively charged carbonyl oxygen atoms tend to escape from this region (e.g., via flipping), due to a strong repulsive electrostatic force imposed by the electrostatic potential valley. When the flipping occurs, the electrostatic potential valley becomes insignificant, indicating that the repulsive electrostatic forces become much weaker, and the structure of selectivity filters should be more stable (**Figure 6(B)** and **Figure 6(D)**). It is noteworthy that, if K^+ ions are present in the selectivity filter, a slightly positive electrostatic potential can be observed, indicating that the carbonyl oxygen atoms are not subject to strong repulsive electrostatic forces (**Figure 6(C)** and **Figure 6(D)**). Therefore, the huge difference in electrostatic potential leads to the distinct stability of the selectivity filter, between systems with and without the presence of K^+ . Indeed,

not restricted to Val76, other residues in the selectivity filter such as Tyr78 also experience reorientation due to the electrostatic repulsion, but however, at a lower extent.

We also calculated the electrostatic potential distributions in the NaK and NavAb channels, as shown in **Figure 6(E)** and **Figure 6(F)**. Prior to the flipping of the Val64 carbonyl oxygen, there is a large and deep electrostatic potential valley in the selectivity filter region of NaK channel (black solid line in **Figure 6(E)**). Just like the situation in KcsA, the induced repulsive electrostatic force on the negatively charged carbonyl oxygen atom results in its flipping. Compared with the KcsA channel, the electrostatic potential valley in NaK channel is less significant (**Figure 6(E)**), and therefore in good agreement with the smaller conformational change of the NaK selectivity filter. In sharp contrast to the KcsA and NaK channels, the electrostatic potential in the NavAb channel does not display significant valleys (**Figure 6(F)**), and as a result, the electrostatic interaction in the selectivity filter region is relatively weak and the structure is stable. In addition, in the presence of coordinated ions, the smooth electrostatic potential profiles for all the three channels (red solid curves in **Figure 6(D)** to **Figure 6(F)**) are consistent with the observation of very high stability in this situation (see **Figure 2(A)**).

3.4. The Role of Hydrogen Bonds

The number and strength of hydrogen bonding networks between residues in the selectivity filter and its adjacent pore helix (especially Glu71) are thought to play an important role in the structural stability of the KcsA selectivity filter [4] [5] [38]. Herein, careful examination of the present simulation trajectories identifies a few key hydrogen bonds closely related to the conformational change process. The backbone amide group of Tyr78 forms a hydrogen bond with the side chain of Glu71 (**Figure 7(A)**); denoted as i), and the backbone amide group of Gly77 forms a hydrogen bond with the carbonyl oxygen in the backbone of Glu71 (denoted as ii). We first calculated the surviving probability of these two hydrogen bonds, before the flipping of Val76. Note that, the simulation trajectory with K^+ in the selectivity filter was used for these calculations, because the trajectory without K^+ in the filter involves very few frames before flipping, and thus cannot offer reliable statistics. We find that the surviving probability of the hydrogen bond ii is 31.85%, significantly lower than the hydrogen bond i at 60.47% (**Figure 7(B)**). Thus, the hydrogen bond ii may first be broken if no ions were present in the selectivity filter, facilitating the flipping of Val76. Meanwhile, the relatively robust hydrogen bond i, the breaking of which is relevant to the narrowing around Gly77, is in agreement with the observation that not all four subunits of the KcsA channel undergo narrowing.

In addition to the hydrogen bonds i and ii, we also identified a previously unnoticed hydrogen bond, formed between the carbonyl group of Val76, in its flipped conformation, and the backbone amide group of Tyr78 (**Figure 7(C)**); denoted as iii). To explore the relevance of this hydrogen bond to the narrowing

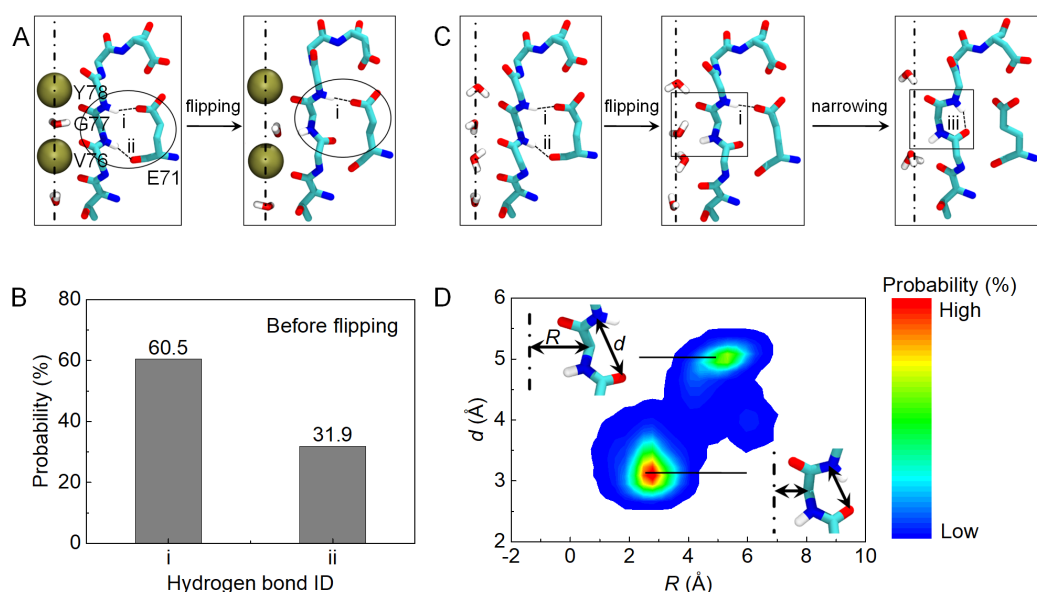


Figure 7. Hydrogen bonding properties of key residues in the KcsA selectivity filter. (A) Schematic of the hydrogen bonds (dashed lines; denoted as i and ii) formed between Gly77 or Val76 and their surroundings. (B) Surviving probability of the hydrogen bonds before the flipping of Val76. (C) Schematic of the hydrogen bond (denoted as iii) between Tyr78 and Val76. The formation of this hydrogen bond is associated with the conformational change at the selectivity filter. (D) Probability distribution of local radius R of the selectivity filter and distance d between the backbone amide nitrogen of Tyr78 (possible donor for the hydrogen bond iii) and carbonyl oxygen of Val76 (possible acceptor).

of selectivity filter, we calculated the probability distribution of local radius R of the selectivity filter and distance d between the backbone amide nitrogen of Tyr78 (possible donor for the hydrogen bond iii) and carbonyl oxygen of Val76 (possible acceptor). The probability distribution map shows two visible spots. The upper right spot is centered at $R = \sim 5.2$ Å and $d = \sim 5$ Å; the large d value impedes the formation of the hydrogen bond iii, and the large R value means the absence of narrowing. In contrast, the lower left spot is centered at $R = \sim 2.7$ Å and $d = \sim 3$ Å; the small d value facilitates the formation of the hydrogen bond iii, and meanwhile, the small R value indicates the occurrence of narrowing.

Because the selectivity filter in the NaK channel shows similar conformational change process with the KcsA channel filter, we discuss below the hydrogen bonds in the NaK channel equivalent to those in the KcsA channel. The backbone amide group of Gly65 forms a hydrogen bond with the backbone carbonyl oxygen of Val59 (**Figure 8(A)**; denoted as i), and the carbonyl group of Val64, in its flipped conformation, forms a hydrogen bond with the backbone amide group of Asp66 (**Figure 8(C)**; denoted as ii). As shown in **Figure 7(B)**, the hydrogen bond i that helps stabilize the Val64 carbonyl oxygen has a higher surviving probability in all four subunits than that in the KcsA channel. This observation is in line with the fact that the NaK channel filter is more stable than the KcsA channel filter. In addition, the hydrogen bond ii is seen to be formed only in chain B which is the sole subunit that undergoes narrowing (**Figure 8(D)**). This result confirms the above observation in the KcsA channel that the

formation of this hydrogen bond is crucial for the narrowing of selectivity filter.

We also inspected the hydrogen bonding networks in NavAb and identified four hydrogen bonds supporting the structure of selectivity filter (**Figure 9**). Note that, different from KcsA and NaK, the simulation trajectory without ions in the NavAb selectivity filter is used for subsequent analysis. The Glu177 side chain of NavAb is supported by an elaborate architecture. The Glu177 side chain

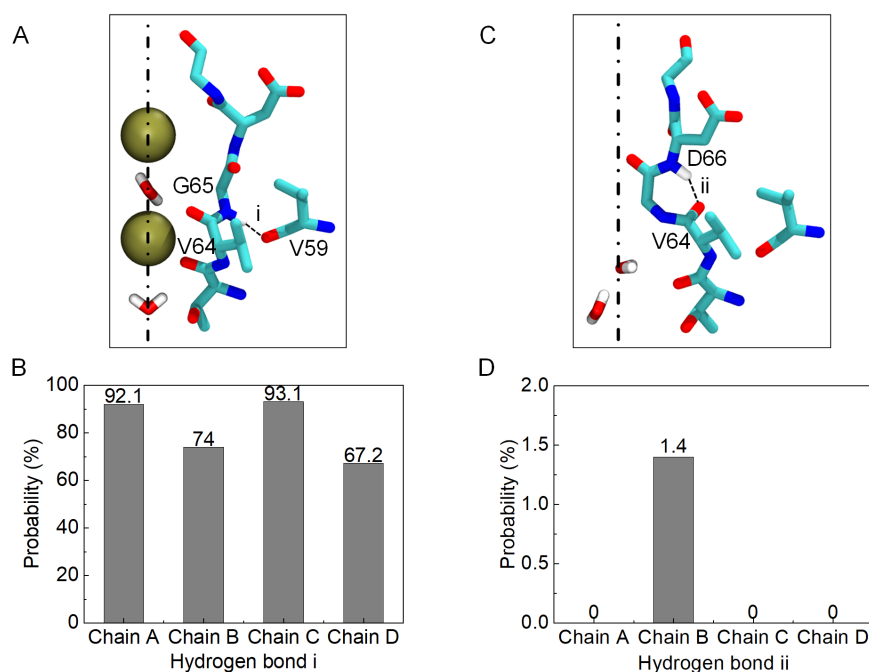


Figure 8. Hydrogen bonding properties of key residues in the NaK selectivity filter. (A) Schematic of the hydrogen bond (denoted as i) between Val64 and their surroundings, monitored in the presence of K⁺ ions inside the filter. (B) Surviving probability of the hydrogen bond i before the flipping of Val64 in all four subunits. (C) Schematic of the hydrogen bond (denoted as ii) between Asp66 and Val64, monitored in the absence of K⁺ ions inside the filter. (D) Surviving probability of the hydrogen bond ii in all four subunits.

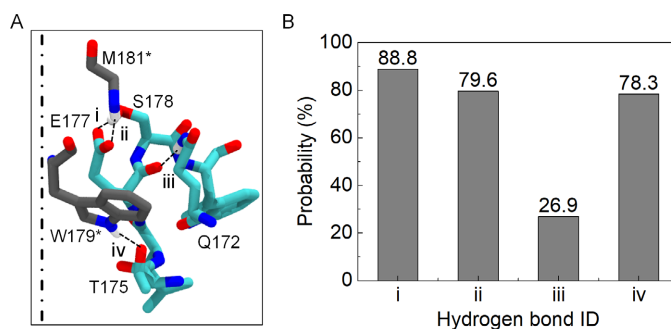


Figure 9. Hydrogen bonding properties of key residues in the NavAb selectivity filter. (A) Schematic of key hydrogen bonds (denoted by i to iv) formed between residues in the selectivity filter and their surroundings. Trp179 and Met181 from the neighbouring subunit are denoted with “*”, with carbon atoms represented in grey. (B) Surviving probability of the four hydrogen bonds in the absence of Na⁺ ions.

forms a hydrogen bond (denoted as i) with the Ser178 side chain, and a hydrogen bond (denoted as ii) with the backbone amide group of Met181 from the neighboring subunit. These two hydrogen bonds stabilize the Glu177 side chain directly. The carbonyl group of Glu177 forms a hydrogen bond (denoted as iii) with the Gln172 side chain, which further stabilizes the selectivity filter. Moreover, the hydrogen bond (denoted as iv) formed by Thr175 and Trp179 in the adjacent subunit forces the Thr175 and Leu176 carbonyls to point toward the pore lumen. Except for the hydrogen bond iii, the surviving probabilities of these key hydrogen bonds are very high (>75%), such that the selectivity filter of NavAb is quite stable even in the absence of Na⁺ ions.

4. Conclusion

We investigate the stability and the underlying mechanism for typical cation channels through extensive molecular dynamics simulations. The stability of the selectivity filter of these typical cation channels in the absence of coordinated ions is inversely correlated with the number of stable binding sites. We show that the distinct repulsive electrostatic forces between negatively charged oxygen atoms that form the stable binding sites are responsible for the different stability in these cation channels. The strong, repulsive electrostatic forces cause a large conformational change in the selectivity filters of the KcsA and NaK channels, in the absence of coordinated ions. The repulsive electrostatic force in the NavAb channel is much weaker, as compared to those for KcsA and NaK, and therefore consistent with the high stability of the filter in this channel. We further show that the hydrogen bonds formed between residues in the selectivity filter and their surroundings helix also play an important role in maintaining structural stability. These results provide important mechanistic insights into the structural stability of the selectivity filters in typical cation channels.

Acknowledgements

This work was supported by the National Key Research and Development Program of China (2019YFA0705400), Natural Science Foundation of Jiangsu Province (BK20212008), the Research Fund of State Key Laboratory of Mechanics and Control of Mechanical Structures (MCMS-I-0421K01), A Project Funded by the Priority Academic Program Development of Jiangsu Higher Education Institutions.

Conflicts of Interest

The authors declare no conflicts of interest regarding the publication of this paper.

References

- [1] Hodgkin, A.L. and Huxley, A.F. (1952). A Quantitative Description of Membrane Current and Its Application to Conduction and Excitation in Nerve. *The Journal of*

- Physiology*, **117**, 500-544. <https://doi.org/10.1113/jphysiol.1952.sp004764>
- [2] Heginbotham, L.; Abramson, T. and Mackinnon, R. (1992). A Functional Connection between the Pores of Distantly Related Ion Channels as Revealed by Mutant K⁺ Channels. *Science*, **258**, 1152-1155. <https://doi.org/10.1126/science.1279807>
- [3] Heginbotham, L.; Lu, Z.; Abramson, T. and Mackinnon, R. (1994). Mutations in the K⁺ Channel Signature Sequence. *Bio-Physical Journal*, **66**, 1061-1067. [https://doi.org/10.1016/S0006-3495\(94\)80887-2](https://doi.org/10.1016/S0006-3495(94)80887-2)
- [4] Doyle, D.A.; Cabral, J.M.; Pfuetzner, R.A.; Kuo, A.; Gulbis, J.M. and Cohen, S.L. *et al.* (1998). The Structure of the Potassium Channel: Molecular Basis of K⁺ Conduction and Selectivity. *Science*, **280**, 69-77. <https://doi.org/10.1126/science.280.5360.69>
- [5] Zhou, Y.; Morais-Cabral, J.H.; Kaufman, A. and MacKinnon, R. (2001). Chemistry of Ion Coordination and Hydration Revealed by a K⁺ Channel-Fab Complex at 2.0 Å Resolution. *Nature*, **414**, 43-48. <https://doi.org/10.1038/35102009>
- [6] Shi, N.; Ye, S.; Alam, A.; Chen, L.P. and Jiang, Y.X. (2006). Atomic Structure of a Na⁺- and K⁺-Conducting Channel. *Nature*, **440**, 570-574. <https://doi.org/10.1038/nature04508>
- [7] Payandeh, J.; Scheuer, T.; Zheng, N. and Catterall, W.A. (2011). The Crystal Structure of a Voltage-Gated Sodium Channel. *Nature*, **475**, 353-358. <https://doi.org/10.1038/nature10238>
- [8] Xu, Y.; Bhate, M.P. and McDermott, A.E. (2017). Transmembrane Allosteric Energetics Characterization for Strong Coupling Between Proton and Potassium Ion Binding in the KcsA Channel. *Proceedings of the National Academy of Sciences*, **114**, 8788-8793. <https://doi.org/10.1073/pnas.1701330114>
- [9] Cuello, L.G.; Jogini, V.; Cortes, D.M. and Perozo, E. (2010). Structural Mechanism of C-type Inactivation in K⁺ Channels. *Nature*, **466**, 203-208. <https://doi.org/10.1038/nature09153>
- [10] Shrivastava, I.H.; Tieleman, D.P.; Biggin, P.C. and Sansom, M.S.P. (2002). K⁺ Versus Na⁺ Ions in a K Channel Selectivity Filter: A Simulation Study. *Biophysical Journal*, **83**, 633-645. [https://doi.org/10.1016/S0006-3495\(02\)75197-7](https://doi.org/10.1016/S0006-3495(02)75197-7)
- [11] Domene, C. and Sansom, M.S.P. (2003). Potassium Channel, Ions, and Water: Simulation Studies Based On the High Resolution X-ray Structure of KcsA. *Biophysical Journal*, **85**, 2787-2800. [https://doi.org/10.1016/S0006-3495\(03\)74702-X](https://doi.org/10.1016/S0006-3495(03)74702-X)
- [12] Furini, S.; Beckstein, O. and Domene, C. (2009). Permeation of Water through the KcsA K⁺ Channel. *Proteins: Structure, Function, and Bioinformatics*, **74**, 437-448. <https://doi.org/10.1002/prot.22163>
- [13] Domene, C. and Furini, S. (2009). Dynamics, Energetics, and Selectivity of the low-K⁺ KcsA Channel Structure. *Journal of Molecular Biology*, **389**, 637-645. <https://doi.org/10.1016/j.jmb.2009.04.038>
- [14] Boiteux, C. and Bernèche, S. (2011). Absence of Ion-Binding Affinity in the Putatively Inactivated Low-[K⁺] Structure of the KcsA Potassium Channel. *Structure*, **19**, 70-79. <https://doi.org/10.1016/j.str.2010.10.008>
- [15] Shen, R. and Guo, W. (2009). Ion Binding Properties and Structure Stability of the NaK Channel. *Biochimica et Biophysica Acta (BBA) - Biomembranes*, **1788**, 1024-1032. <https://doi.org/10.1016/j.bbamem.2009.01.008>
- [16] Shen, R.; Guo, W. and Zhong, W. (2010). Hydration Valve Controlled Non-Selective Conduction of Na⁺ and K⁺ in the NaK Channel. *Biochimica et Biophysica Acta (BBA) - Biomembranes*, **1798**, 1474-1479. <https://doi.org/10.1016/j.bbamem.2010.04.002>

- [17] Qiu, H.; Shen, R. and Guo, W. (2012). Ion Solvation and Structural Stability in a Sodium Channel Investigated by Molecular Dynamics Calculations. *Biochimica et Biophysica Acta (BBA) - Biomembranes*, **1818**, 2529-2535. <https://doi.org/10.1016/j.bbamem.2012.06.003>
- [18] Cordero-Morales, J.F.; Cuello, L.G.; Zhao, Y.; Jogini, V.; Cortes, D.M. and Roux, B. *et al.* (2006). Molecular Determinants of Gating at the Potassium-Channel Selectivity Filter. *Nature Structural & Molecular Biology*, **13**, 311-318. <https://doi.org/10.1038/nsmb1069>
- [19] Cordero-Morales, J.F.; Jogini, V.; Lewis, A.; Vasquez, V.; Cortes, D.M. and Roux, B. *et al.* (2007). Molecular Driving Forces Determining Potassium Channel Slow Inactivation. *Nature Structural & Molecular Biology*, **14**, 1062-1069. <https://doi.org/10.1038/nsmb1309>
- [20] Cordero-Morales, J.F.; Jogini, V.; Chakrapani, S. and Perozo, E. (2011). A Multi-point Hydrogen-Bond Network Underlying KcsA C-type Inactivation. *Biophysical Journal*, **100**, 2387-2393. <https://doi.org/10.1016/j.bpj.2011.01.073>
- [21] Ostmeyer, J.; Chakrapani, S.; Pan, A.C.; Perozo, E. and Roux, B. (2013). Recovery from Slow Inactivation in K⁺ Channels is Controlled by Water Molecules. *Nature*, **501**, 121-124. <https://doi.org/10.1038/nature12395>
- [22] Li, J.; Ostmeyer, J.; Cuello, L.G.; Perozo, E. and Roux, B. (2018). Rapid Constriction of the Selectivity Filter Underlies C-type Inactivation in the KcsA Potassium Channel. *Journal of General Physiology*, **150**, 1408-1420. <https://doi.org/10.1085/jgp.201812082>
- [23] Ranatunga, K.M.; Shrivastava, I.H.; Smith, G.R. and Sansom, M.S.P. (2001). Side-Chain Ionization States in a Potassium Channel. *Biophysical Journal*, **80**, 1210-1219. [https://doi.org/10.1016/S0006-3495\(01\)76097-3](https://doi.org/10.1016/S0006-3495(01)76097-3)
- [24] Bernèche, S. and Roux, B. (2002). The Ionization State and the Conformation of Glu-71 in the KcsA K⁺ Channel. *Biophysical Journal*, **82**, 772-780. [https://doi.org/10.1016/S0006-3495\(02\)75439-8](https://doi.org/10.1016/S0006-3495(02)75439-8)
- [25] Bucher, D.; Guidoni, L. and Rothlisberger, U. (2007). The Protonation State of the Glu-71/Asp-80 Residues in the KcsA Potassium Channel: A First-Principles QM/MM Molecular Dynamics Study. *Biophysical Journal*, **93**, 2315-2324. <https://doi.org/10.1529/biophysj.106.102509>
- [26] Phillips, J.C.; Braun, R.; Wang, W.; Gumbart, J.; Tajkhorshid, E. and Villa, E. *et al.* (2005). Scalable Molecular Dynamics with NAMD. *Journal of Computational Chemistry*, **26**, 1781-1802. <https://doi.org/10.1002/jcc.20289>
- [27] Humphrey, W.; Dalke, A. and Schulten, K. (1996). VMD: Visual Molecular Dynamics. *Journal of Molecular Graphics*, **14**, 33-38. [https://doi.org/10.1016/0263-7855\(96\)00018-5](https://doi.org/10.1016/0263-7855(96)00018-5)
- [28] MacKerell, A.D.; Bashford, D.; Bellott, M.; Dunbrack, R.L.; Evanseck, J.D. and Field, M.J. *et al.* (1998). All-Atom Empirical Potential for Molecular Modeling and Dynamics Studies of Proteins. *The Journal of Physical Chemistry B*, **102**, 3586-3616. <https://doi.org/10.1021/jp973084f>
- [29] MacKerell, A.D.; Feig, M. and Brooks, C.L. (2004). Improved Treatment of the Protein Backbone in Empirical Force Fields. *Journal of the American Chemical Society*, **126**, 698-699. <https://doi.org/10.1021/ja036959e>
- [30] Best, R.B.; Zhu, X.; Shim, J.; Lopes, P.E.M.; Mittal, J. and Feig, M. *et al.* (2012). Optimization of the Additive CHARMM All-Atom Protein Force Field Targeting Improved Sampling of the Backbone Φ , Ψ and Side-Chain X_1 and X_2 Dihedral Angles. *Journal of Chemical Theory and Computation*, **8**, 3257-3273.

- <https://doi.org/10.1021/ct300400x>
- [31] Klauda, J.B.; Venable, R.M.; Freites, J.A.; O'Connor, J.W.; Tobias, D.J. and Mondragon-Ramirez, C. *et al.* (2010). Update of the CHARMM All-Atom Additive Force Field for Lipids: Validation on Six Lipid Types. *The Journal of Physical Chemistry B*, **114**, 7830-7843. <https://doi.org/10.1021/jp101759q>
- [32] Beglov, D. and Roux, B. (1994). Finite Representation of an Infinite Bulk System - Solvent Boundary Potential for Computer-Simulations. *Journal of Chemical Physics*, **100**, 9050-9063. <https://doi.org/10.1063/1.466711>
- [33] Jorgensen, W.L.; Chandrasekhar, J.; Madura, J.D.; Impey, R.W. and Klein, M.L. (1983). Comparison of Simple Potential Functions for Simulating Liquid Water. *The Journal of Chemical Physics*, **79**, 926-935. <https://doi.org/10.1063/1.445869>
- [34] Essmann, U.; Perera, L.; Berkowitz, M.L.; Darden, T.; Lee, H. and Pedersen, L.G. (1995). A Smooth Particle Mesh Ewald Method. *The Journal of Chemical Physics*, **103**, 8577-8593. <https://doi.org/10.1063/1.470117>
- [35] Feller, S.E.; Zhang, Y.; Pastor, R.W. and Brooks, B.R. (1995). Constant Pressure Molecular Dynamics Simulation: The Langevin Piston Method. *The Journal of Chemical Physics*, **103**, 4613-4621. <https://doi.org/10.1063/1.470648>
- [36] Aksimentiev, A. and Schulten, K. (2005). Imaging α -Hemolysin with Molecular Dynamics: Ionic Conductance, Osmotic Permeability, and the Electrostatic Potential Map. *Biophysical Journal*, **88**, 3745-3761. <https://doi.org/10.1529/biophysj.104.058727>
- [37] Almers, W. and Armstrong, C.M. (1980). Survival of K^+ Permeability and Gating Currents in Squid Axons Perfused with K^+ -Free Media. *Journal of General Physiology*, **75**, 61-78. <https://doi.org/10.1085/jgp.75.1.61>
- [38] Bernèche, S. and Roux, B. (2000). Molecular Dynamics of the KcsA K^+ Channel in a Bilayer Membrane. *Biophysical Journal*, **78**, 2900-2917. [https://doi.org/10.1016/S0006-3495\(00\)76831-7](https://doi.org/10.1016/S0006-3495(00)76831-7)